JOURNAL OF COLLOID AND INTERFACE SCIENCE **182,** 465–472 (1996)
ARTICLE NO. 0489

Dynamic and Equilibrium Phase Behavior in the $C_{12}E_5$–Abietic Acid–H_2O System

STEPHEN P. BEAUDOIN,[1] RUBEN G. CARBONELL,[2] AND CHRISTINE S. GRANT

Department of Chemical Engineering, North Carolina State University, Raleigh, North Carolina 27695

Received March 8, 1995; accepted April 17, 1996

Previous research has investigated the removal of representative flux residues (abietic acid (AA) in isopropyl alcohol (IPA)) from printed wiring assemblies using aqueous solutions of a nonionic surfactant (pentaethylene glycol mono-*n*-dodecyl ether ($C_{12}E_5$)). To optimize cleaning with this surfactant, greater understanding of the equilibrium and dynamic phase behavior in the AA-$C_{12}E_5$-H_2O system is required. In this research, partial ternary phase diagrams were developed at 60 and 45°C (above the binary cloud point). Increasing the AA content of the system caused isotropic surfactant (L2) and lamellar liquid crystalline (La) phases to form at lower temperatures than in the binary $C_{12}E_5$–H_2O system. As the temperature increased, the solubility of AA in the L2 phase increased considerably, while the AA content of the La phase was not affected as strongly. The dynamic phase behavior resulting from contact of micellar $C_{12}E_5$ solutions with AA or AA/IPA particles at 24°C (below the binary cloud point) and 45°C was also observed. When AA or AA/IPA particles were contacted with 4.1×10^{-3} *M* $C_{12}E_5$ solutions, the surfactant and water penetrated into the particles to create isotropic liquid aggregates. When particles were contacted with more concentrated micellar $C_{12}E_5$ solutions (0.25 *M*), a new concentrated surfactant phase surrounded the particles and solubilized the AA. © 1996 Academic Press, Inc.

Key Words: **micelles; nonionic surfactants; surfactant phase behavior; detergency; solubilization.**

INTRODUCTION

The removal of solid films of abietic acid (AA) containing up to 45% isopropyl alcohol (IPA) from disks of FR-4 epoxy–glass laminate (Fig. 1) by aqueous solutions of a nonionic surfactant (pentaethylene glycol mono-*n*-dodecyl ether, $C_{12}E_5$) has been studied under controlled hydrodynamic conditions (1, 2). This work resulted from a need to eliminate the use of CFC-113-based solutions to remove flux residues from printed wiring assemblies (PWAs). FR-4 laminate is a common substrate used in PWAs, while the mixture of AA and IPA is representative of flux residue. The studies identified a multistage cleaning mechanism consisting of the following steps: (1) surfactant and water penetration into the AA/IPA, (2) shear-driven removal of an AA–surfactant–water liquid phase, and (3) shear-driven removal of isolated AA–surfactant–water aggregates directly from the FR-4 surface.

In emulsification-based cleaning of liquid oily soils from surfaces, the first step is adsorption and penetration of surfactant into the contaminant (4–7). The surfactant and water then mix with the oil (contaminant) phase to form water-in-oil or oil-in-water emulsions. Droplets of these emulsions may be displaced from the surface by hydrodynamic forces. These steps are consistent with the cleaning observed in the $C_{12}E_5$–water–AA system.

The research presented here investigates the dynamic and equilibrium behavior observed when particles and films of AA/IPA are contacted with aqueous solutions of $C_{12}E_5$ at several temperatures. These investigations enhance understanding of the cleaning process by allowing the phases formed to be related to the controlling parameters seen in the cleaning. This also facilitates optimization of cleaning conditions for the removal of flux residues from PWAs using aqueous surfactant solutions.

EXPERIMENTAL PROCEDURES

Materials

The AA used in this study was supplied by Alfa Specialty Chemicals and was approximately 90% pure. Its density was determined to be 1.08 g/ml by comparison with sucrose solutions of known density. The IPA and tetrahydrofuran (THF) (Fisher Chemicals) were HPLC grade, and the $C_{12}E_5$ (Nikko Chemicals of Japan) was 99% pure, as verified by gas chromatography at Nikko. All chemicals were used as received. The water used in this work was 18.3 MΩ-cm DI water from a Barnstead Nanopure system.

Equilibrium Phase Diagrams

To construct ternary AA–$C_{12}E_5$–water phase diagrams, mixtures of $C_{12}E_5$, water, and AA were allowed to equilibrate

---

[1] Current address: Arizona State University, Dept. of Chemical, Bio., and Materials Engineering, Tempe, AZ 85287.

[2] To whom correspondence should be addressed.

0021-9797/96 $18.00

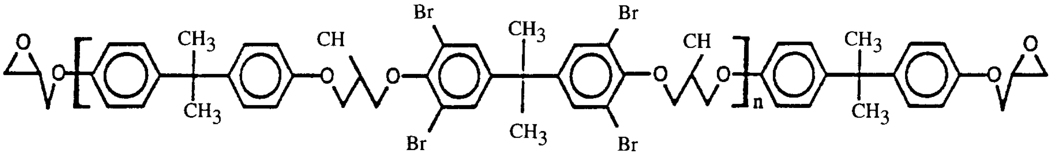

FIG. 1. Brominated epoxy resin typical of FR-4 (3).

for periods ranging from three weeks to two months at constant temperature in a Fisher Isotemp Model 615A oven. The solutions were held in tapered, airtight vials of Teflon-PFA (Cole–Parmer) during the equilibration. The vials were agitated vigorously at least once each day so that all phases were well mixed. Optical microscopy was used to determine the equilibrium phase structures of the samples, and their compositions were determined using gel-permeation chromatography. Phases were sampled with a 1 ml Hamilton Gas-Tight syringe. Approximately half of each sample was placed in a new glass capillary tube (VitroDynamics; 0.8 mm path length, 8 mm width, rectangular capillaries; flame-sealed at one end) for analysis of its phase structure. The remainder of each sample was used to determine its composition (discussed below). Between sampling and analysis, each capillary tube was maintained at the equilibrium temperature in a Fisher recirculating water bath, although the lag time between sampling and analysis was always less than 5 min. The samples were studied at 100× magnification under both unpolarized and polarized light using an optical microscope (Olympus BH-P) equipped with an Olympus C-35 AD2 camera and photographic system. A red filter was used to assist in the detection of birefringence and to identify the rotation of Maltese crosses in the lamellar liquid crystalline (La) phase (8, 9). A hot stage (Sensortek TS-4 ER Controller and Hot Stage) was used to maintain the capillaries at the equilibrium temperature during viewing. Phases were identified by comparing their optical characteristics (birefringence, oily streaks, Maltese crosses) to those of representative surfactant phases (8, 9). The presence of AA was inferred from the yellow–brown–orange color of the phases.

To determine the phase compositions, the second portion of each phase sample (see above) was placed in a preweighed glass vial with a Teflon-lined screw top lid (Fisher), and the mass was recorded. In the initial stages of the work, these samples were freeze-dried using a Virtis 10-324 lyophilization apparatus, and their water content was determined by the change in mass during drying. The samples were then dissolved in THF and analyzed using gel-permeation chromatography (GPC) to determine their AA content. With this method, a THF mobile phase was pumped through three μStyragel columns (1000, 100, and 10 Å pore diameter) in series using a Waters 6000A Isocratic Pump. A Waters 440 UV Absorbance Detector (UV detector) set at 254 nm was placed downstream of the columns to detect the AA. The UV detector was calibrated using solutions of known AA concentration. A Rheodyne injector with a 200 μl liquid-phase injection loop was used for sample injection. Thus, the water and AA contents of the phases were measured, and the $C_{12}E_5$ content was determined by total mass balance.

In later stages of the work, the lyophilization was omitted and the samples were dissolved directly in THF and injected into the GPC apparatus. In this case, a 1000 Å μStyragel column and two Shodex kf-801 GPC columns in series were used for the separation and a Waters 410 Differential Refractometer (RI apparatus) was placed downstream of the UV detector. The RI apparatus was calibrated against $C_{12}E_5$ solutions of known concentration. In this method, the AA and $C_{12}E_5$ contents of the solution were measured and the water content was determined by mass balance. Replicate samples analyzed by both methods showed good agreement, although there was less variation between samples analyzed by the second method.

Dynamic Phase Behavior

The dynamic behavior of aqueous $C_{12}E_5$ solutions in contact with pure AA or AA/IPA particles was studied using the optical microscope at 100× magnification. AA particles were obtained directly from the material provided by Alfa, while mixed AA/IPA particles were obtained from AA/IPA films on disks of FR-4 laminate. These films were made when 42% (mass) solutions of AA in IPA were spin-coated onto FR-4 disks using a Headway Research, Model CB15 spin-coating apparatus (1, 2). After drying in a desiccator for 24 h, these films were less than 4 μm thick. A razor blade was used to scrape the dried film samples from the disks. The particles (AA or AA/IPA) were placed on a glass microscope slide with a cover slip, and aqueous $C_{12}E_5$ solution was placed at the edges of the cover slip using a clean 1 ml Hamilton Gas-Tight syringe. The surfactant solutions flowed under the cover slip to contact the particles. The contacting was observed through the microscope and photographs were taken to document changes in both the particles and the aqueous solution with time. An excess of surfactant solution was maintained at the edges of the cover slip during contacting, and the slide was maintained at the desired temperature using a hot stage. Prior to addition to the slides, the surfactant solutions were maintained at the contacting temperature using a Fisherbrand Recirculating

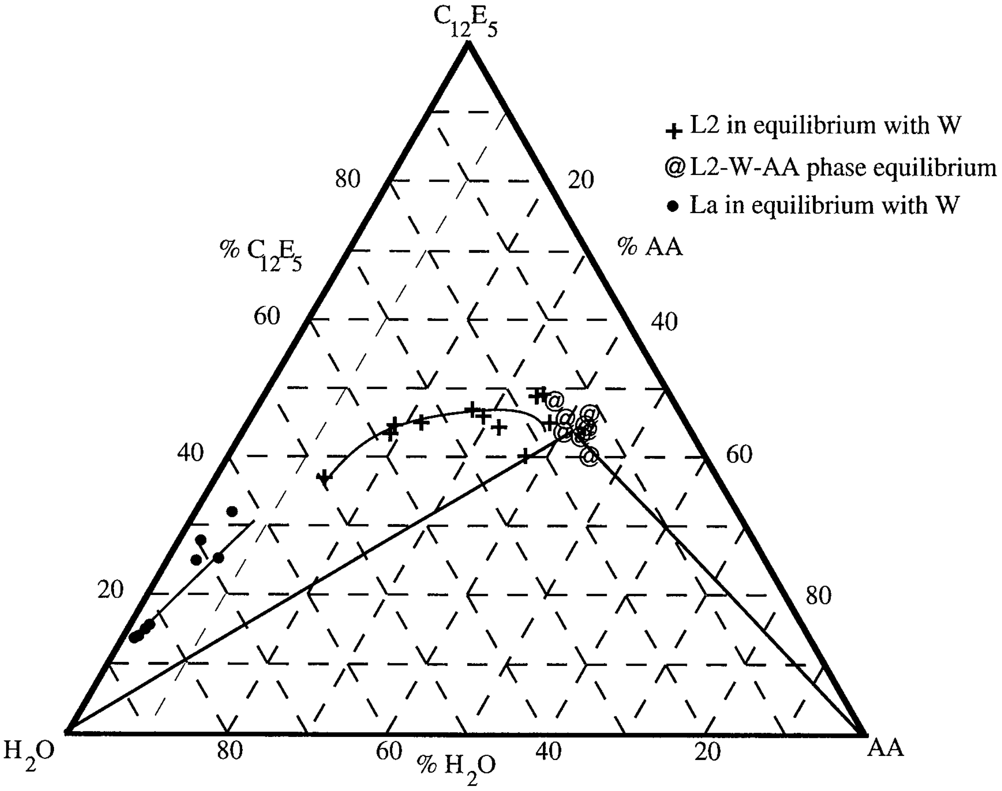

FIG. 2. Ternary $C_{12}E_5$–AA–H_2O phase diagram at 60°C. La = lamellar liquid crystalline phase containing solubilized AA; L2 = isotropic surfactant liquid containing solubilized AA; S = solid AA; W = dilute aqueous phase.

Water Bath. To search for characteristics of the La phase, the polarized lenses of the microscope were crossed and a red filter was employed. The microscope stage was tilted during the contacting to see if flow birefringence (a characteristic of the sponge-like liquid crystal (L3) phase) was exhibited by any of the phases.

RESULTS AND DISCUSSION

Equilibrium Phase Diagrams at 60 and 45°C

The partial phase diagrams obtained for the H_2O-$C_{12}E_5$-AA system at 60 and 45°C are presented in Figs. 2 and 3. The regions of extremely low surfactant or AA concentration were not investigated. Also, surfactant and water contents of the solid phases of each diagram were not evaluated. It was assumed that the solid was pure AA.

Comparison of Figs. 2 and 3 reveals that the L2 phase forms at 60°C in the presence of approximately 12 to 42% AA in solution and at lower AA levels at 45°C. At these surfactant concentrations, the L2 phase does not form in the binary system below approximately 82°C, although it is seen at 60°C when the surfactant content of the system is greater than roughly 80% by mass (10). At 45°C, the L2–W–AA vertex (which represents the solubility limit of AA in the L2 phase) is below the point of equal solubilization of water and AA, although it is above the point of equal solubilization at 60°C. The range of compositions in the La–W system at 45°C is similar to that seen in the 60°C case, indicating that the effect of temperature on the composition of this phase is small.

To further investigate the effect of AA on the phase transitions in the ternary system, the effect of AA on the cloud point of a micellar $C_{12}E_5$ solution was studied. The CMC of $C_{12}E_5$ at 24°C is 6.4×10^{-5} *M*, and is insensitive to small temperature changes (6). A 4.1×10^{-3} *M* $C_{12}E_5$ solution without AA had a cloud point of 32.5°C, while 1.4×10^{-4} *M* AA in the same solution reduced the cloud point to 29.5°C. Other researchers also have found that oils in water–surfactant systems cause a change in the cloud point (11, 12). The reductions in the temperatures of the cloud point and of L2 phase formation indicate that AA makes aqueous $C_{12}E_5$ solutions more hydrophobic.

When the concentration of AA in the La phase was high, this phase was denser than the W phase, and when the concentration of AA in the La phase was low, the W phase was denser. In the regions of W–L2–solid AA phase equilibrium (above ~42% AA in solution at 60°C; above ~18% AA in solution at 45°C), the solid AA was the densest phase. The L2 phase was always more dense than the W phase, whether they were present in a two- or three-phase system. The L2

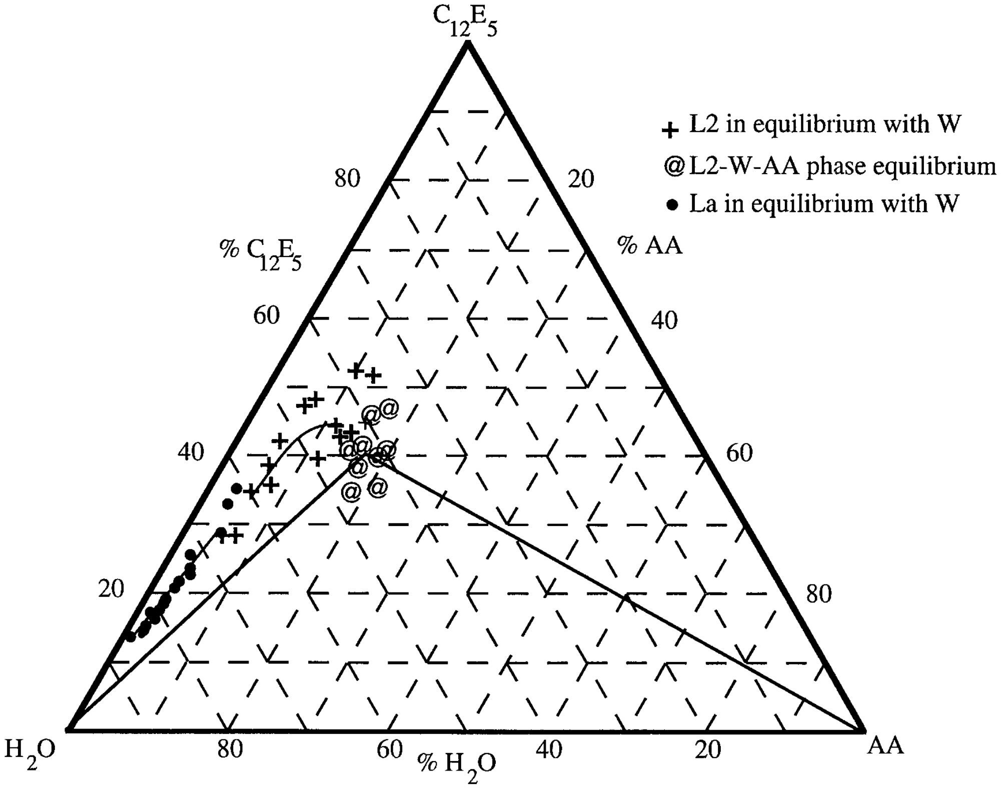

FIG. 3. Ternary $C_{12}E_5$–AA–H_2O phase diagram at 45°C. La = lamellar liquid crystalline phase containing solubilized AA; L2 = isotropic surfactant liquid containing solubilized AA; S = solid AA; W = dilute aqueous phase.

phase was usually clear, in contrast to the La phase, which was usually turbid.

Figure 4 is a photograph (in polarized light) of the La phase containing solubilized AA at 60°C. One unit step on the grid in Figure 4 is equal to 15 μm (as for all photographs in this paper). The Maltese crosses on the right-hand side

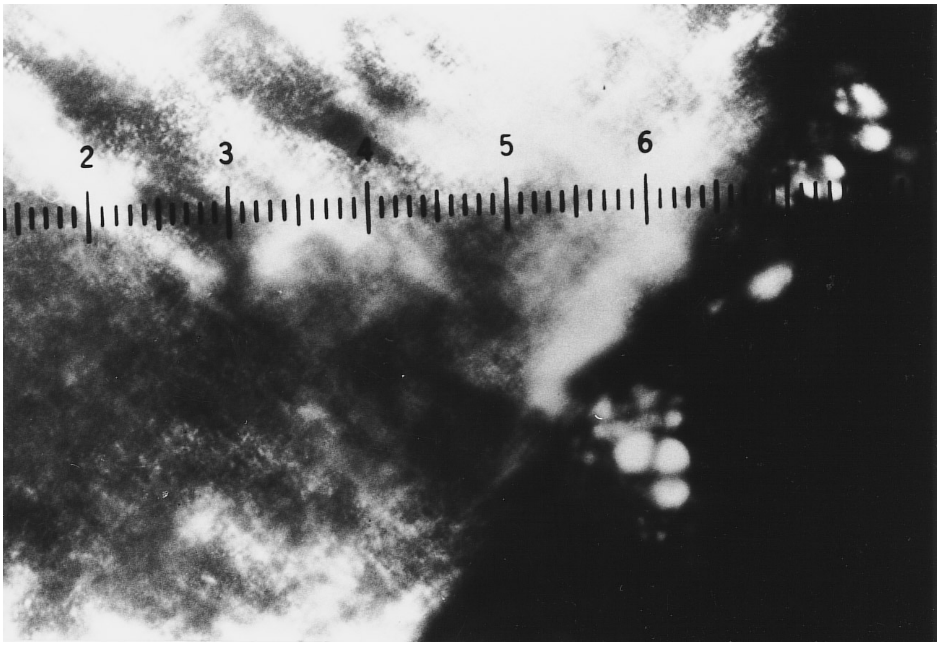

FIG. 4. Photograph of La phase containing solubilized AA; 60°C, approximately 20% (wt) $C_{12}E_5$, 5% (wt) AA, 75% (wt) H_2O.

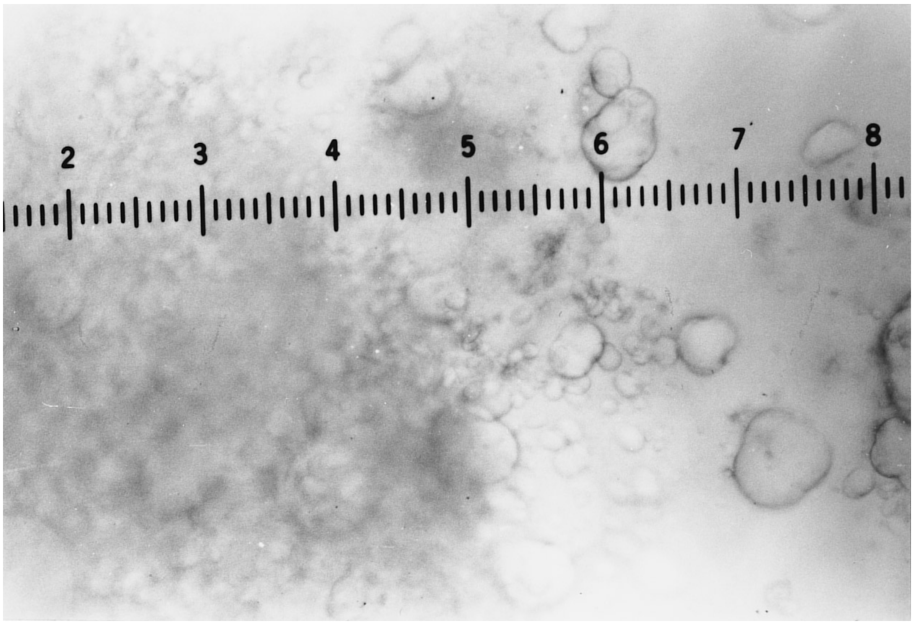

FIG. 5. Photograph of L2 phase containing solubilized AA; 60°C, approximately 45% (wt) $C_{12}E_5$, 40% (wt) AA, 15% (wt) H_2O.

of Fig. 4 and the streaky birefringence on the left-hand side of this photo are characteristic of the La phase (13).

The L2 phase occasionally contained roughly spherical internal structures, as shown in Fig. 5 (60°C, unpolarized light). No birefringent regions were detected in this phase, and it did not exhibit flow birefringence. The spheres are thought to be regions of local order. They showed no tendency to move out of the bulk phase, even when it was dispersed into the W phase by vigorous mixing. The spheres had the same color and texture as the bulk phase, and the number and size of the spheres were not affected by the intensity or frequency of mixing. These observations suggest that the spheres were not emulsified water droplets, but were characteristic of this L2 phase.

Dynamic Phase Behavior

Figure 6 presents photographs of the contacting of 1×10^{-3} M (in unpolarized light) and 0.25 M (in polarized light) $C_{12}E_5$ solutions with AA particles at 24°C. Figure 7 presents photographs (in unpolarized light) of the contacting of 4.1×10^{-3} M $C_{12}E_5$ solutions with AA/IPA particles (45 wt% IPA) at 24 and 45°C. The photos show that when aqueous solutions of $C_{12}E_5$ contact AA or AA/IPA particles at either temperature, the surfactant and water penetrate and liquefy the particles. Emulsions did not form in the liquefied organic phase at either temperature, although a concentrated surfactant phase formed on the particles when 0.25 M $C_{12}E_5$ was used. This is seen in Fig. 6D, where a birefringent surfactant phase (possibly La) formed at the outer edge of the particle. This layer, which appeared transiently during the contact, solubilized AA and then broke from the interface and streamed into the bulk solution (not shown). No solubilization in the aqueous phase was observed at any condition in the absence of concentrated surfactant layers such as this. In the 1×10^{-3} M photos (Figs. 6A, 6B), the size of the AA/$C_{12}E_5$ aggregates increased during the liquefaction, suggesting that water penetrated into the surfactant-laden AA.

As the temperature increased, the rate of liquefaction of the AA/IPA particles increased, as shown in Fig. 7. It has been shown that the saturation concentration of $C_{12}E_5$ in AA/IPA films increases with increasing temperature (1, 2), perhaps due to a reduction in the solubility of the surfactant in the aqueous phase (14). This may explain the increased rate of penetration at 45°C. Although the diffusion coefficients for surfactant and water in both the organic and aqueous phases is thought to increase with increasing temperature, it is unlikely that this effect alone accounted for the change in liquefaction rate.

Figures 6 and 7 at 24°C show that the liquefaction of the AA/IPA particles occurred in the same manner as for the pure AA particles. However, the IPA reduced slightly the time required to liquefy the particles. This may have been due to an increased affinity of the surfactant and water for particles containing IPA.

When AA/IPA particles were contacted with 0.25 M $C_{12}E_5$ at 24 and 45°C, the liquefaction was so rapid that no photographs could be taken. The liquefied organic also swelled rapidly before breaking up and becoming solubilized in solution, presumably due to the penetration of surfactant and water. During the liquefaction, there was rapid streaming of surfactant solution towards the AA/IPA particles, which dissolved into the streaming fluid. This high rate of liquefac-

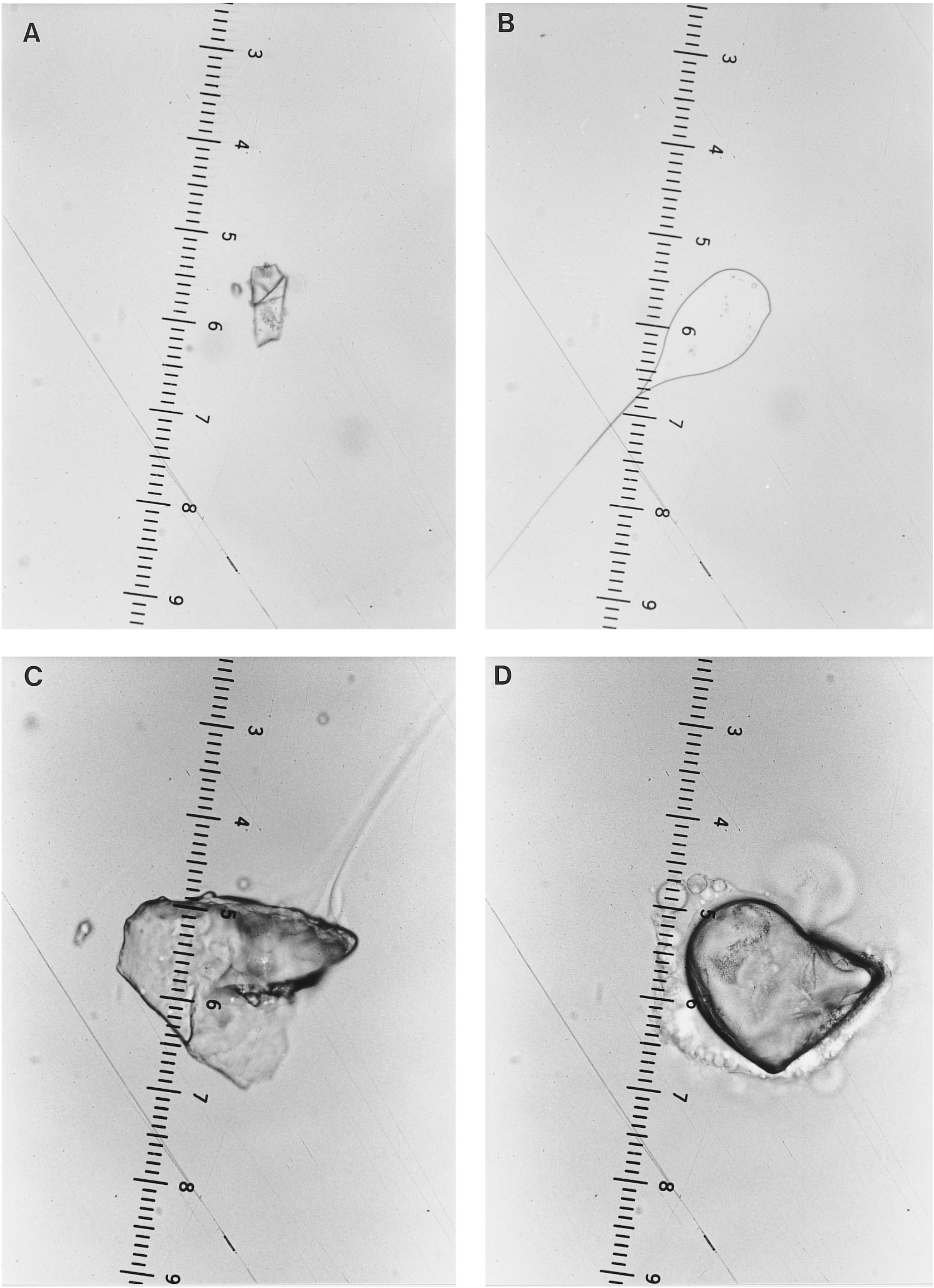

FIG. 6. Contact results, 24°C. A, B: 1×10^{-3} *M* $C_{12}E_5$ with AA particle, unpolarized light; C, D: 0.25 *M* $C_{12}E_5$ with AA particle, polarized light (A at contact, B 94 min; C at contact, D 4 min).

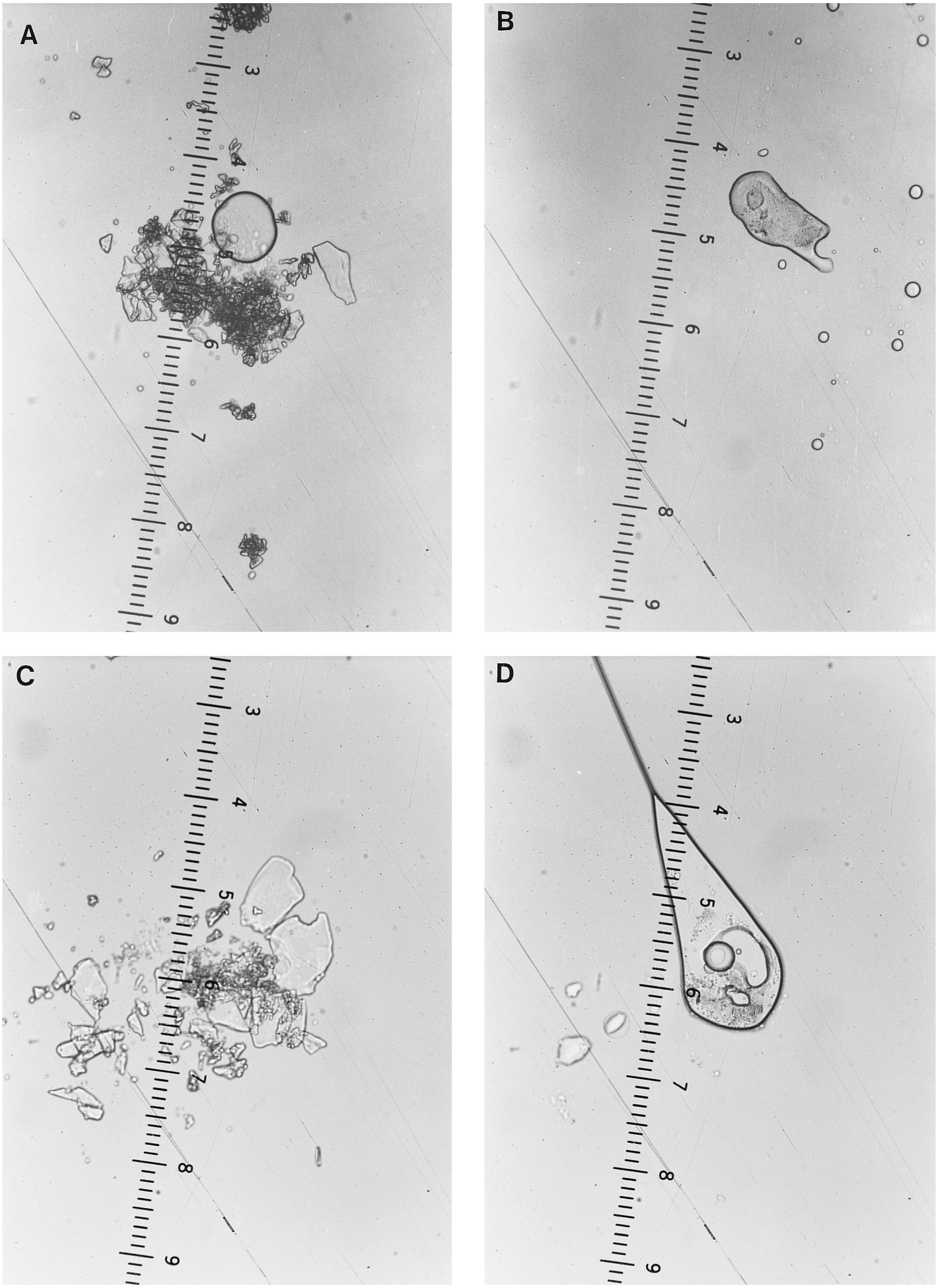

FIG. 7. Contact results, 4.1×10^{-3} *M* $C_{12}E_5$ with AA/IPA particle. A, B: 24°C; C, D: 45°C (A at contact, B 79 min: C at contact, D 13 min.)

tion may have been due to the formation of concentrated surfactant phases at the water/particle interface (as in Fig. 6D), although the effect of micelles also may have been important. It has been postulated that the controlling step in the removal of oil drops from polymer fibers by nonionic surfactant solutions is the rate of dissociation of micelles and the subsequent adsorption of their molecularly dissolved surfactant molecules onto the oil (15, 16). The large number of micelles in the 0.25 *M* solutions may have increased the liquefaction rate by enhancing this penetration step.

CONCLUSIONS

The presence of AA in aqueous solutions of $C_{12}E_5$ induced the formation of L2 phases at temperatures significantly below those required in the binary surfactant–water system. The solubility limit of AA in the L2 phase was significantly higher at 60° than at 45°C, although the solubility limit in the La phase was not strongly affected by temperature over this range.

When $C_{12}E_5$ solutions contact AA or AA/IPA particles, the primary action of the surfactant is to liquefy them. Only under conditions of extremely high surfactant concentration does detectable solubilization of the particles occur. This is consistent with cleaning results presented elsewhere (1, 2). Combined with results of those cleaning studies, the experimental results presented here offer a more complete picture of the process of surfactant-based cleaning than was previously available, by allowing the phases formed during the cleaning process to be related to the rates of their removal.

ACKNOWLEDGMENTS

The authors thank Northern Telecom Co. in Research Triangle Park, North Carolina for providing FR-4 laminate, and AT&T in Princeton, New Jersey and Digital Equipment Corp. in Augusta, Maine for their assistance in planning this work. Funding for this work was received from the Pollution Prevention Research Center at North Carolina State University and from the National Science Foundation Program for Environmentally Benign Chemical Synthesis and Processing (Grant CTS-9216850). The authors acknowledge Christine Palmer, Stacey Julien, and Rochelle Carlton for their assistance in the laboratory.

REFERENCES

1. Beaudoin, S. P., Carbonell, R. G., and Grant, C. S., *Ind. Eng. Chem. Res.* **34,** 3307 (1995).
2. Beaudoin, S. P., Carbonell, R. G., and Grant, C. S., *Ind. Eng. Chem. Res.* **34,** 3318 (1995).
3. Wang, D. W., *in* ‘‘Electronic Packaging Materials Science III,’’ Materials Research Society Symposia Proceedings, Vol. 108, p. 125. Mater. Res. Soc., New York, 1988.
4. Cox, M. F., *J. Am. Oil Chem. Soc.* **63**(4), 1559 (1990).
5. Cox, M. F., Smith, D. L., and Russell, G. L., *J. Am. Oil Chem. Soc.* **64**(2), 273 (1987).
6. Rosen, M. J., ‘‘Surfactants and Interfacial Phenomena.’’ Wiley, New York, 1989.
7. Scheuing, D. R., *Langmuir* **6,** 312 (1990).
8. Hartshorne, N. H., ‘‘The Microscopy of Liquid Crystals.’’ Microscope Publications, Chicago, 1974.
9. Taupin, C., Auvray, L., and Di Meglio, M. R., ‘‘Micellar Solutions and Microemulsions.’’ Springer-Verlag, New York, 1990.
10. Mitchell, D. J., Tiddy, G. J. T., Waring, L., Bostock, T., and McDonald, M. P., *J. Chem. Soc. Faraday Trans.* **179,** 975 (1983).
11. Schambil, F., and Schwuger, M. J., *Colloid Polym. Sci.* **265**(11), 1009 (1987).
12. Miller, C. A., and Raney, K. H., *Colloids Surf. A.* **74,** 169 (1993).
13. Hartshorne, N. H., and Stuart, A., ‘‘Crystals and the Polarizing Microscope,’’ 4th ed. Edward Arnold, London, 1970.
14. Myers, D., ‘‘Surfactant Science and Technology.’’ VCH, New York, 1988.
15. Carroll, B. J., *J. Colloid Interface Sci.* **79,** 126 (1981).
16. Carroll, B. J., O’Rourke, G. C., and Ward, J. I., *J. Pharm. Pharmacol.* **34,** 287 (1982).